

**Supplementary Figure 1 - Additional correlations with published MCM ChIP-seq, ORC ChIP-seq, origin timing and origin efficiency data sets.**

(A) The correlation between the firing time of origins, as determined by the firing-time parameter  $n$  from a quantitative analysis of replication kinetics (Yang et al., 2010), and the number of MCM ChIP-seq reads in a 1 kb window around those origins taken from an immunoprecipitation with an anti-Mcm2-7 polyclonal antibody (Belsky et al., 2015). See D for correlation coefficients. (B) The same analysis as in A for an Mcm4-5FLAG immunoprecipitation (De Piccoli et al., 2012). (C) The correlation between the number of ORC ChIP-seq reads (Eaton et al., 2010) and the number of MCM ChIP-seq reads (from our data) in a 1 kb window around origins. Pearson's coefficient ( $r$ ) for the correlation is 0.43. (D) Pearson's correlation coefficients for all pair-wise combinations of datasets analyzed. “All origins” refers to all 335 origins identified by Yang et al. (Yang et al., 2010); non-chromatin-influenced origins are those whose timing is not affected by telomere proximity (Lian et al., 2011), Rpd3 (Knott et al., 2009), Fkh1 (Knott et al., 2012); Ctf19 (Natsume et al., 2013).

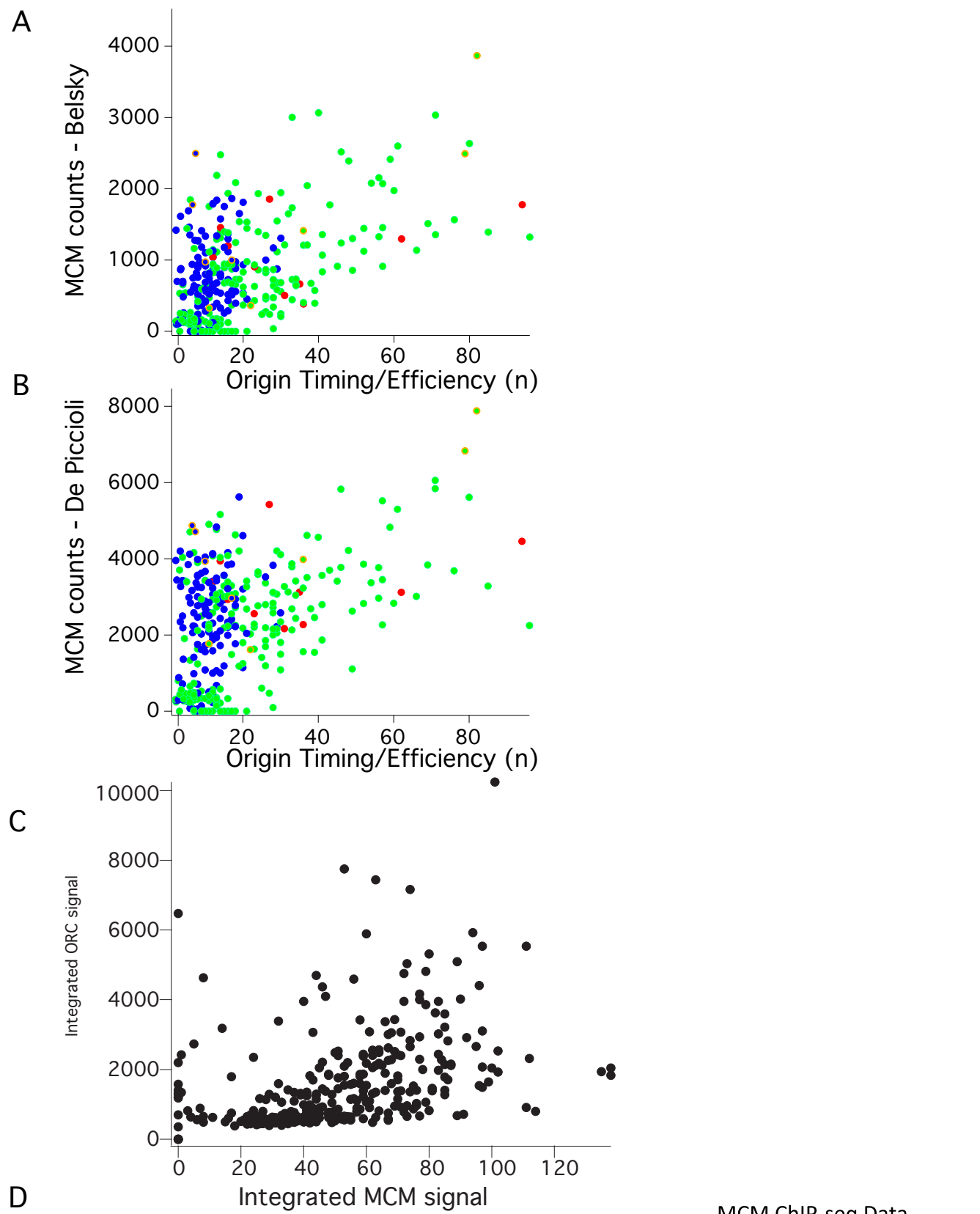
**Supplementary Figure 2 - Additional TALO8 plasmid-purification experiments.**

(A) Diagram of the TALO8 system. Above: a graphic representation of the TALO8 plasmids used. Below: a graphic representation of the TALO8 plasmid bound to LacI, ORC, MCM and Zif268. Graphics are not to scale. (B) Specificity controls for the TALO8 westerns. TALO8 plasmid was purified from cells with Mcm2 (yFS847), Orc2 (yFS848) or both (yFS849) C-terminally HA tagged and expressed from their endogenous genes, and wild-type cells expressing HA-tagged Zif268 (yFS852). TALO8-bound proteins were analyzed by HA western. (C) HA western of ARS305-TALO8-bound proteins from G1-arrested Mcm2-HA, Orc2-HA, Zif268-HA cells (yFS861). (D) Quantitation of data in C.

**Supplementary Figure 3- Additional data for replication timing experiments.**

(A) Replication progress as analyzed by flow cytometry for representative wild-type (yFS833) and ARS1- $\Delta$ B2 (yFS842) time courses used in Figure 3C. (B) Quantitation of all four time courses analyzed in Figure 3C. The average replication time for these cultures, which differ due to experimental variation, was used to normalize the NanoString data. (C) Data for the wild-type strain (yFS833) analyzed as in Figure 3C, but normalized independently of the ARS1- $\Delta$ B2 strain (yFS842) to allow the timing of ARS1 to be directly compare to other origins in that strain. However, because bulk replication in the ARS1- $\Delta$ B2 strain is later, it is not appropriate to compare absolute replication times with out the normalization applied in Figure 3C. Instead, it is possible to compare relative replication times. Relative to the other measured origins, ARS1 replicates at 0.31 of the way through S, whereas ARS1 $\Delta$ B2 replicates at 0.68. Omitting ARS1218 (which has high variance in the two experiments) ARS1 replicates at 0.13 and ARS1 $\Delta$ B2 replicates at 0.34. (D) Data from the ARS1- $\Delta$ B2 strain (yFS842) analyzed as in C. (E) The correlation between the NanoString-based replication timing data and published deep-sequencing-based replication timing data (Hawkins et al., 2013; McGuffee et al., 2013).

# Figure S1



MCM ChIP-seq Data	
Das	Belsky
0.42	0.54
0.54	0.61
0.47	0.49
0.50	0.54
0.46	0.46
0.47	0.48
	0.44
	0.58
	0.43
	0.46
	0.42
	0.44

Timing/Efficiency Data	Origins Analyzed	Das	Belsky	De Piccioli
Yang	All	0.42	0.54	0.44
	Non-chromatin-influenced	0.54	0.61	0.58
McGuffee	All	0.47	0.49	0.43
	Non-chromatin-influenced	0.50	0.54	0.46
Hawkins	All	0.46	0.46	0.42
	Non-chromatin-influenced	0.47	0.48	0.44

# Figure S2

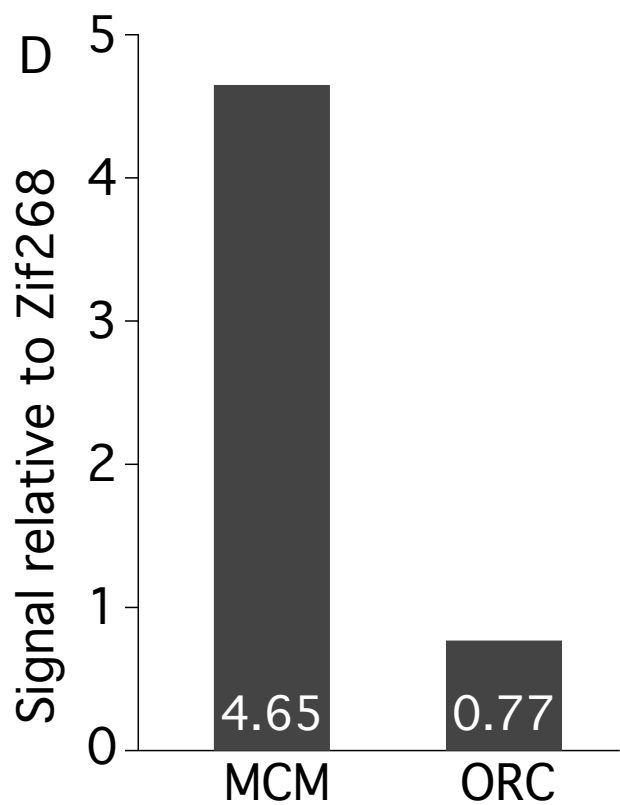
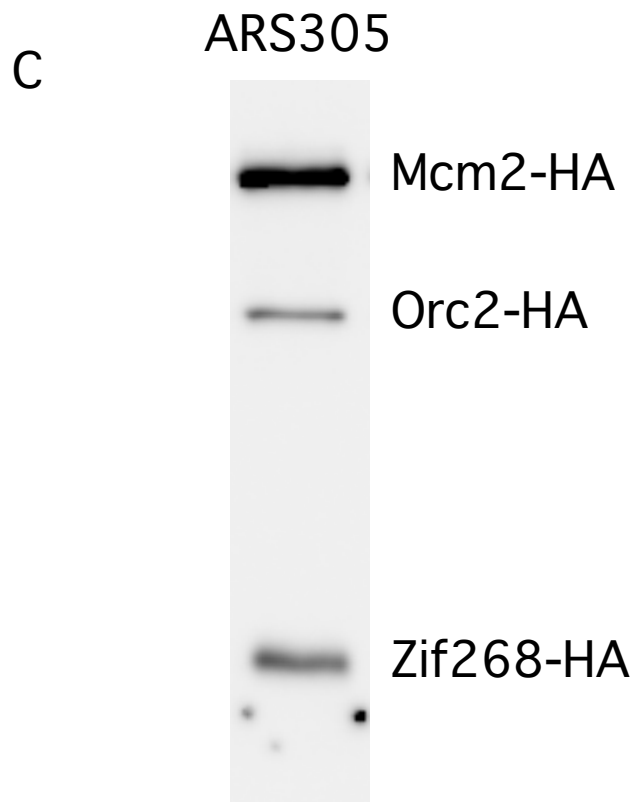
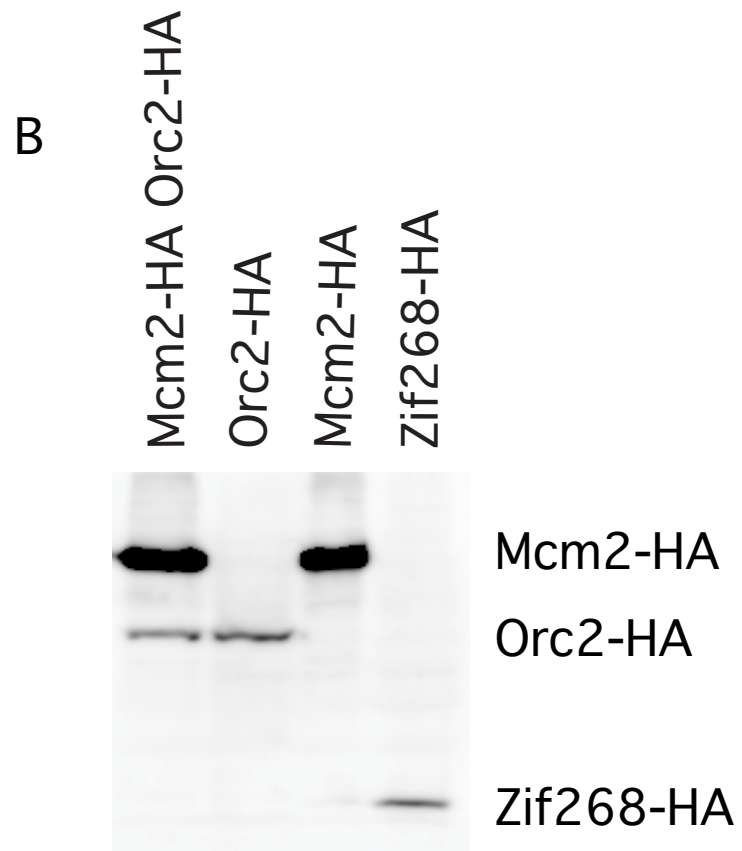
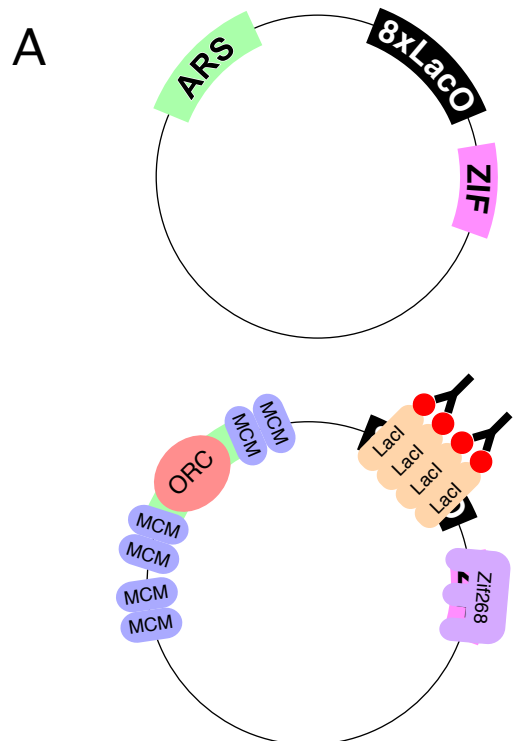
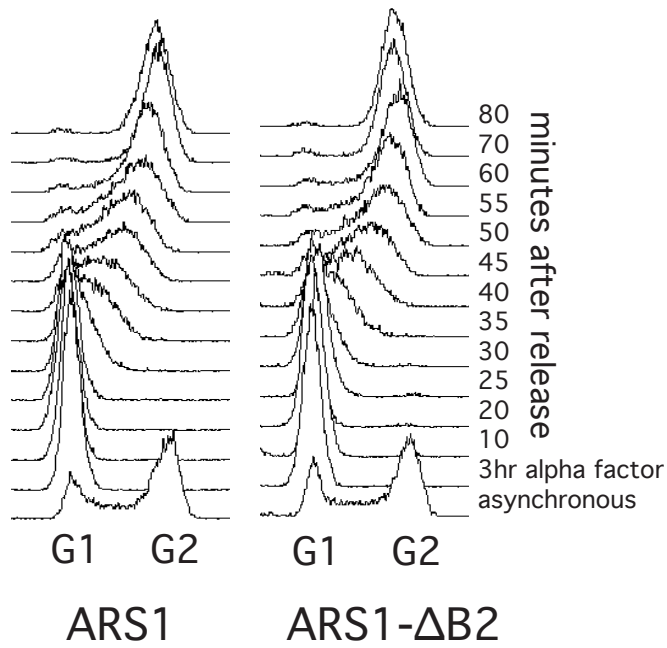
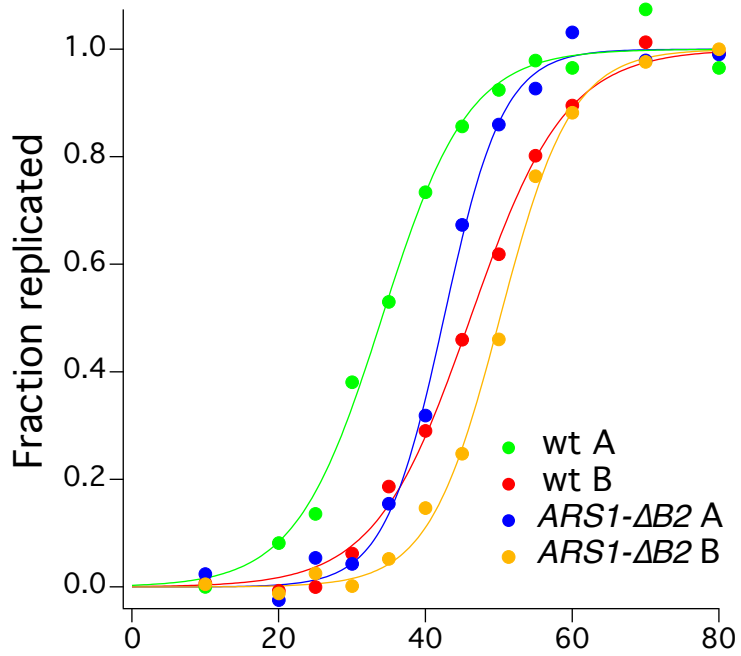


# Figure S3

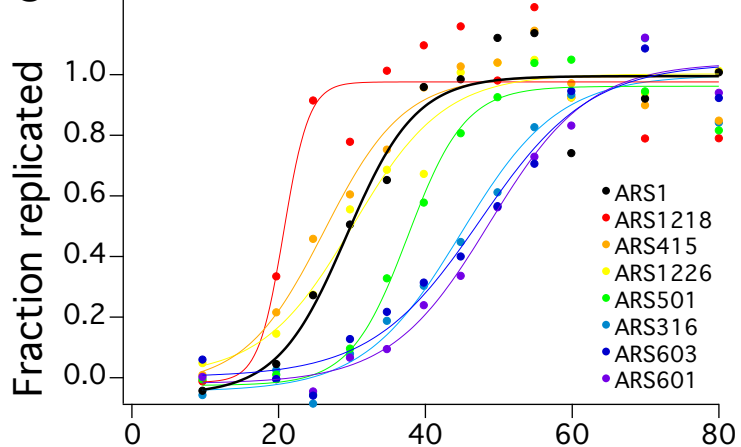
A



B



C



D

